Electronic Supplementary Material (ESI) for Catalysis Science & Technology.

Hydrogen reverse spillover eliminating methanation over efficient Pt-Ni catalysts for water-gas shift reaction

Jing Lyu[a], Ye Tian[a, *], Yingtian Zhang[a], Peipei Wu[a], Yu Pan[a], Tong Ding[a], Song Song[a], and Xingang Li[a, b, *]

[a] Collaborative Innovation Center of Chemical Science and Engineering (Tianjin), State Key Laboratory of Chemical Engineering, Tianjin Key Laboratory of Applied Catalysis Science and Engineering, School of Chemical Engineering & Technology, Institute of Shaoxing, Tianjin University, Tianjin, 300350, P. R. China

[b] School of Chemistry and Chemical Engineering, Lanzhou Jiaotong University, Lanzhou, Gansu, 730070, P. R. China

1. Catalysts preparation

1.1. Materials

$Ni(NO_3)_2 \cdot 6H_2O$ was purchased from Adamas Reagent, Ltd., and the purity of the product is 99 wt.%. The ammonia aqueous solution ($NH_3 \cdot H_2O$) with an NH_4^+ concentration of 25 wt.% was brought from Macklin Inc.. The silica sol containing 25 wt.% SiO_2 was purchased from Qingdao Ocean Chemical Co. Ltd.. $NaBH_4$ (GR) was purchased from Tianjin Jiangtian Chemical Technology Co. Ltd..

1.2. Catalysts preparation

The Ni phyllosilicate containing 20 wt.% nickel was prepared by the ammonia evaporation method. 5.6 g of $Ni(NO_3)_2 \cdot 6H_2O$ was dissolved in distilled water, and a 25 wt.% aqueous ammonia solution (NH_3/Ni molar ratio = 8) was added dropwise. After stirring the mixture for 15 minutes, 18 g of silica sol was introduced in it. The mixture was stirred for 2 h. The initial pH of the nickel ammonia complex solution was 11~12. All procedures mentioned above were conducted at room temperature. Next, the suspension was moved in a water bath preheated at 90 °C to evaporate ammonia and deposit nickel species on silica. The evaporation process ended up when the pH value decreased to 7. The resultant precipitate was filtered and washed by distilled water and anhydrous ethanol to remove the remaining ammonium ions. The green precipitate was dried at 100 °C for 12 h. The dried solid was milled into powder and calcinated at 600 °C for 4 h in a muffle furnace. The acquired sample was denoted as NiPS-P. NiPS-P was reduced at 500 °C for 1 h, and the acquired catalyst was denoted as Ni/NiPS.

Pt was loaded on NiPS-P by the impregnation method. 655 μL of H_2PtCl_6 water solution (0.0395 mol L^{-1}) was added to 50 mL of water, and the solution was sonicated for 10 min. Then 1.0 g of NiPS-P was dispersed in the solution, and the mixture was sonicated for 20 min. The mixture was evaporated at 60 °C by a rotary evaporator and further dried in a drying oven at 80 °C. The dried solid was milled into powder and calcinated at 600 °C for 4 h. The Pt loading amount was 0.5 wt.%, and the prepared sample was denoted as Pt/NiPS-P. Pt/NiPS-P was reduced at 500 °C for 1 h, and the acquired catalyst was denoted as Pt-Ni/NiPS.

Pt/SiO_2 was prepared by the conventional impregnation method. 655 μL of H_2PtCl_6 water solution (0.0395 mol L^{-1}) was added to 50 mL of water, and the solution was sonicated for 10 min. Then we added 1.0 g of SiO_2 powder in it. The SiO_2 powder originated from the comprehensively dried silica sol. The mixture was evaporated at 60 °C and then was dried at 80 °C for 12 h. The dried solid was milled into powder and calcinated at 600 °C for 4 h. The acquired sample was denoted as Pt/SiO_2-P. Pt/SiO_2-P was reduced at 500 °C for 1 h, and the acquired catalyst was denoted as Pt/SiO_2.

Ni/SiO_2 was prepared by the conventional impregnation method. 2.5 g of $Ni(NO_3)_2 \cdot 6H_2O$ was dissolved in 50 mL of distilled water, and then we added 2.0 g of SiO_2 powder in it. The SiO_2 powder originated from the comprehensively dried silica sol. The mixture was evaporated at 60 °C and then was dried at 80 °C for 12 h. The dried solid was milled into powder and calcinated at 600 °C for 4 h. The acquired sample was denoted as Ni/SiO_2-P. Ni/SiO_2-P was reduced at 500 °C for 1 h, and the acquired catalyst was denoted as Ni/SiO_2.

Pt-Ni/SiO_2 was prepared by the impregnation method. 655 μL of H_2PtCl_6 water solution (0.0395 mol L^{-1}) was added to 50 mL of water, and the solution was sonicated for 10 min. Then 1.0 g of Ni/SiO_2-P was dispersed in the solution, and the mixture was sonicated for 20 min. The mixture was evaporated at 60 °C and further dried at 80 °C. The dried solid was milled into powder and calcinated at 600 °C for 4 h. The Pt loading amount was 0.5 wt.%, and the prepared sample was denoted as Pt-Ni/SiO_2-P. Pt-Ni/SiO_2-P was reduced at 500 °C for 1 h, and the acquired catalyst was denoted as Pt-Ni/SiO_2.

Pt/NiPS was prepared by chemical reduction method. 500 mg of NiPS-P and 325 μL of H_2PtCl_6 water solution (0.0395 mol L^{-1}) were added in 80 mL of water. The mixture was sonicated for 10 min. 240 mL of $NaBH_4$ was added to 2 mL of NaOH water solution (0.4 g L^{-1}) to acquire $NaBH_4$ solution. The $NaBH_4$ solution was added to the mixture dropwise and the mixture was stirred for 1 h. After stirring, the mixture was washed by water for 3 times. Then, the washed solid was dried at 60 °C in vacuum. The dried solid was calcinated at 500 °C for 1 h in N_2 atmosphere and the calcinated solid was denoted as Pt/NiPS.

2. Catalysis activity test

The water-gas shift reaction (WGSR) activity tests were conducted at atmospheric pressure in a continuous-flow stainless steel reactor (inner diameter = 8 mm) in a vertical furnace. The prepared samples were pressed, milled and sieved to achieve the catalyst particles between 60 and 100 mesh for the kinetic tests. Before the tests, the catalysts were pretreated at 500 °C in a 20 vol.% H_2/80 vol.% N_2 gas flow with a total flow rate of 55 mL min^{-1} for 1 h. The tests were carried out in a 5 vol.% CO/10 vol.% H_2O/85 vol.% N_2 gas flow. The WHSV of kinetic tests was 1,800,000 mL g_{cat}^{-1} h^{-1}. The products were analyzed online by a gas chromatograph (Agilent 7890A) equipped with two thermal conductivity detectors (TCD): one is used to monitor gas species including CO_2, N_2, CH_4 and CO, and the other one is used for H_2 monitor. The CO conversion was calculated by equation Eq. (1), and the CH_4 selectivity was calculated by equation Eq. (2).

$$\text{CO conversion} = \frac{\text{H}_{2\text{flow rate}_{out}} + \text{H}_{2\text{flow rate}_{out}}}{\text{CO}_{\text{flow rate}_{in}}} \times 100\% \#(1)$$

$$\text{CH}_{4\text{selectivity}} = \frac{\text{CH}_{4\text{flow rate}_{out}}}{\text{H}_{2\text{flow rate}_{out}} + \text{CH}_{4\text{flow rate}_{out}}} \times 100\% \#(2)$$

The reaction rate was calculated by Eq. (3). The unit of the mass of catalyst is gram, and the unit of time is second.

$$r = \frac{\text{mole of CO converted to H}_2}{\text{mass of catalyst} \times \text{time}} \#(3)$$

Arrhenius equation shown in Eq. (4) was used to calculate the activation energy (E_a) and the pre-exponential factor (A). k represents the rate constant, and R represents the universal gas constant. The unit of T is Kelvin.

$$k = Ae^{-\frac{E_a}{RT}} \#(4)$$

TOF was calculated by Eq. (5).

$$TOF = \frac{\text{number of moles of CO converted per second}}{\text{number of moles of surface Ni atoms}} \#(5)$$

The number of CO converted per second was calculated according to the kinetic results and the CO conversion was lower than 10%. The Ni dispersion (D) was calculated by an empirical formula: $D = 0.97/d$[1], where d represents the average particle size of the catalysts and its value is given in TEM results. The number of moles of surface Ni atoms was calculated by Eq. (6).

$$\text{Number of moles of surface Ni atoms} = \text{total mole of Ni species} \times \text{reduction degree} \times D \#(6)$$

Total mole of Ni species was calculated according to the catalyst weight of kinetic test. The reduction degree of Ni was calculated in Fig. S3.

3. Characterization

The Brunauer-Emmett-Teller (BET) surface areas and pore structure of the catalysts were gauged by a QuadraSorb SI Physisorption Analyser at −196 °C. All BET tests were conducted after degas for 3 h. The specific surface area was calculated by BET method, and the pore size distribution was calculated by the Barrett-Joyner-Halenda (BJH) method.

The X-ray fluorescence analysis (XRF) experiments were conducted on a Bruker S4 Pioneer in a bid to acquire the chemical element content of the catalysts.

The transmission electron microscopy (TEM) images were obtained on a JEOL JEM 2100F system, which was operated at the accelerating voltage of 200 kV and equipped with a field emission gun. The catalyst was dispersed in anhydrous ethanol by sonication, and then the suspension was dropped on the support films.

The X-ray diffraction (XRD) patterns were recorded with a Bruker D8 Focus operating at 40 mA and 40 kV, using a Cu Kα radiation source (λ = 0.15418 nm). The scan rate was 8 ° min^{-1}.

The H_2 temperature-programmed reduction (H_2-TPR) experiments were conducted on a TPDRO apparatus (TP-5080, Tianjin Xianquan Co. Ltd) equipped with a TCD behind a solid trap to determine the hydrogen consumption. Before the experiment, 80 mg of the sample was loaded in a quartz tube and heated to 200 °C in 30 mL min^{-1} of N_2 gas to remove the surface physically adsorbed water. After cooling down to the room temperature, the sample was heated from ambient temperature to 900 °C with a ramp rate of 10 °C min^{-1}.

The X-ray photoelectron spectroscopy (XPS) analysis was conducted in Thermo Fischer ESCALAB 250Xi with Al Kα 1486.6 eV radiation as the excitation source. Before the experiments, the samples were reduced at 500 °C for 1 h and preserved in vacuum condition. The binding energies (BE) were calibrated using the C 1s peak (BE = 284.8 eV) as a standard and were quoted with a precision of 0.1 eV.

In situ diffuse reflectance infrared Fourier transform spectroscopy (in situ DRIFTS) spectra were executed using a Harrick HVC high temperature transmission cell with a ZnSe window. The reduction process was proceeded in 8 vol.% H_2/N_2 atmosphere, and the CO adsorption process was implemented in 7 vol.% CO/N_2 atmosphere. The water pre-adsorption was carried out by N_2 passing through water at 55 °C

to carry water vapor.

The hydrogen temperature-programmed desorption (H_2-TPD) experiments were conducted on TP-5080. The gas was analyzed by HPR-20. The reduction process and the H_2 pre-adsorption process were carried out in 8 vol.% H_2/N_2 atmosphere at 500 °C, and then the catalysts was cooled to ambient temperature in 8 vol.% H_2/N_2 atmosphere. The H_2 desorption process was conducted successively in N_2 atmosphere. The H_2 desorption process was conducted at ambient temperature for 70 min and then heated to 200 °C (5 °C min^{-1}).

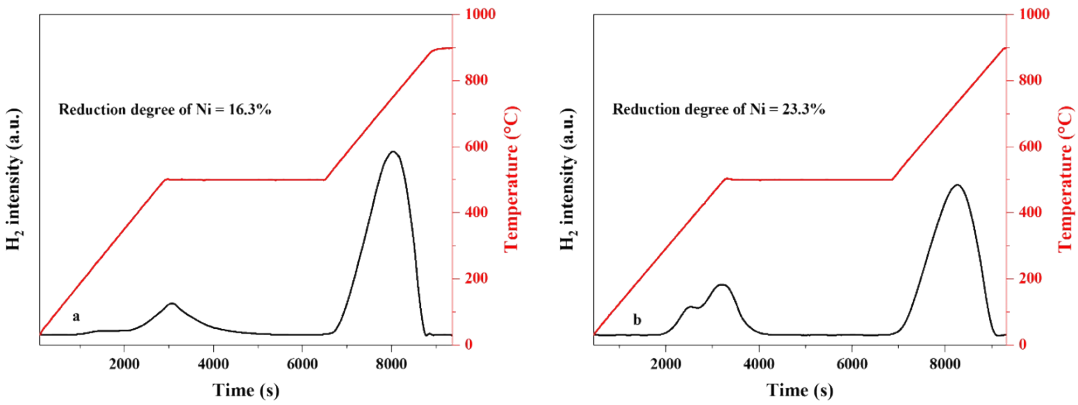

Fig. S1. H_2-TPR profiles with the temperature program of constant at 500 ℃ for 1 h of (a) NiPS-P and (b) Pt/NiPS-P.

The temperature program of constant at 500 ℃ for 1 h was added to TPR experiments in order to calculate the reduction degree of the catalysts. The reduction degree of the catalysts at 500 ℃ was calculated by equation Eq. (7), and presented in Fig. S1. S_1 represents the TPR peak area from ambient temperature to 500 °C and constant at 500 °C for 1 h. S_{total} represents the sum of all TPR peak area.

$$\text{reduction degree} = \frac{S_I}{S_{total}} \quad (7)$$

According to the reduction degree, the Ni^0 loading on Ni/NiPS and Pt-Ni/NiPS was calculated as 3.3 wt.% and 4.7 wt.%, respectively.

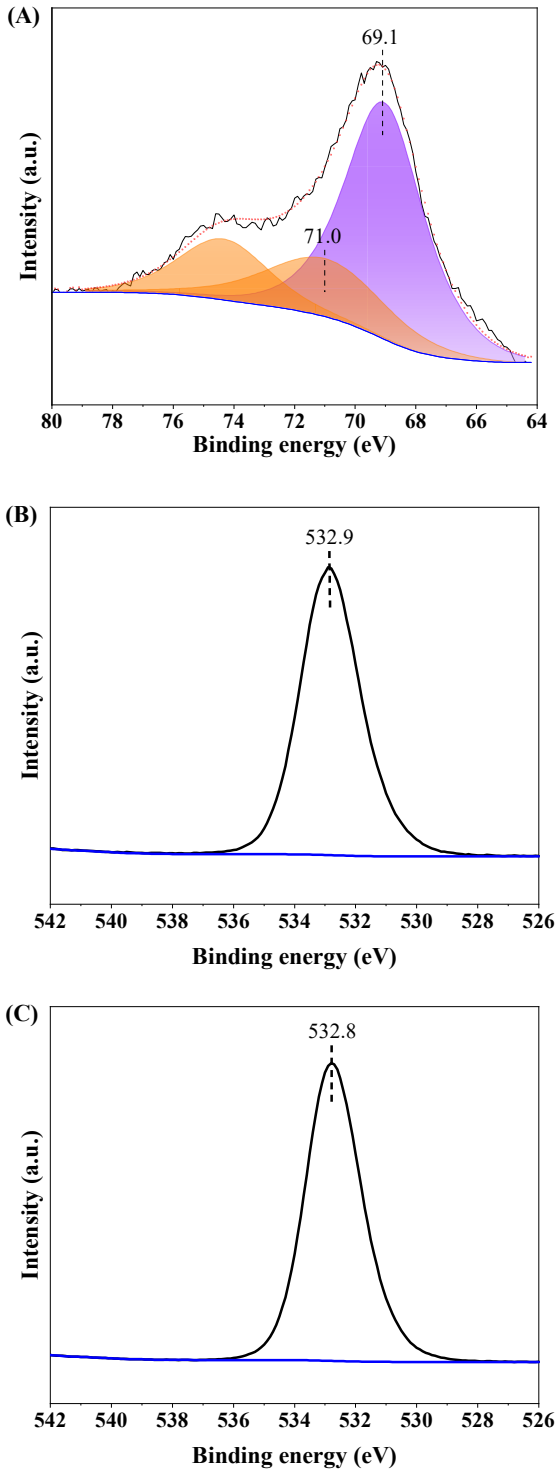

Fig. S2. (A) Pt 4f XPS spectrum of Pt-Ni/NiPS and O 1s XPS spectra of (B) Pt-Ni/NiPS and (C) Ni/NiPS.

In Fig. S2A, 69.1 eV and 71.0 eV are attributed to Ni 3p and Pt $4f_{7/2}$, respectively[2]. In Fig. S2B and C, the peak around 532.8 eV is assigned to the O 1s of SiO_2[3].

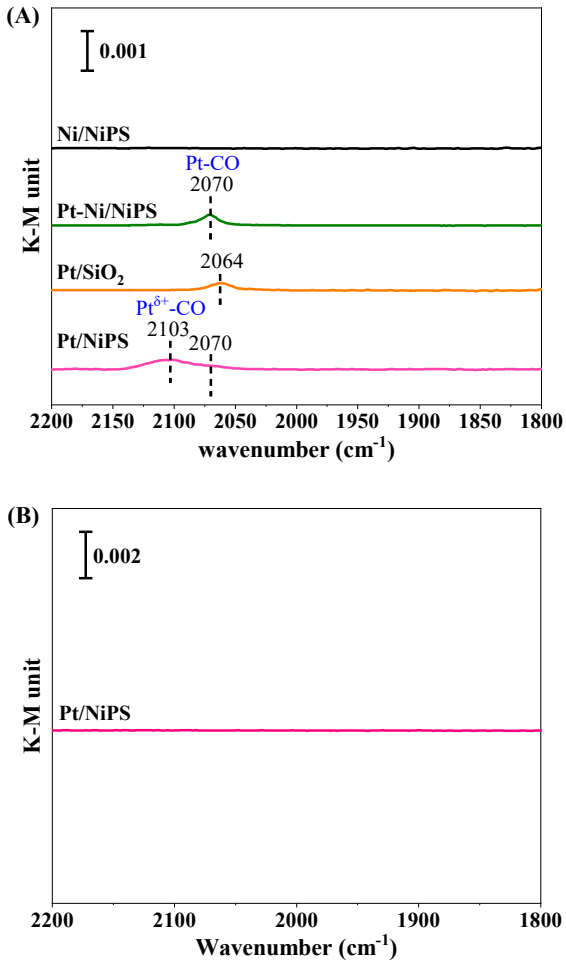

Fig. S3. In situ DRIFTS of CO adsorption at (A) 100 °C and (B) 300 °C for 15 min purged by N_2 for 10 min for the catalysts.

According to previous works, the peaks around 2070 cm^{-1} are attributed to CO linear adsorption on Pt^0 [4]. And the peak at 2103 cm^{-1} can be assigned to CO linear adsorption on $Pt^{\delta+}$ [5].

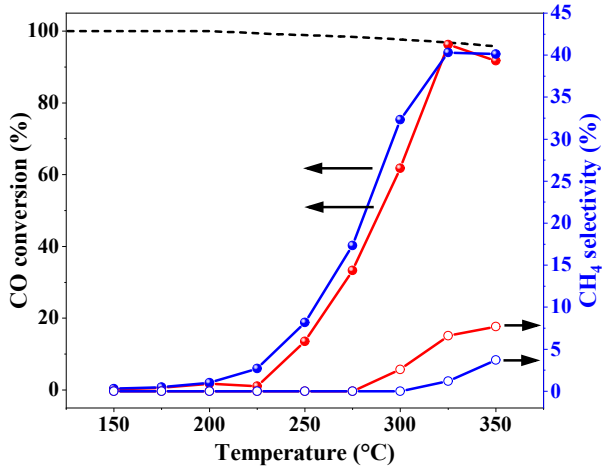

Fig. S4. CO conversion and CH_4 selectivity over the catalysts at WHSV of 36,000 mL g^{-1} h^{-1}. Dashed line: theoretical CO equilibrium conversion. Feed gas: 5% CO, 10% H_2O and N_2 balanced. Red line and ball stand for Ni/SiO_2. Blue line and ball stand for $Pt\text{-}Ni/SiO_2$.

For comparison, we evaluated the WGSR activity of Ni/SiO_2 and $Pt\text{-}Ni/SiO_2$ prepared by impregnation method in Fig. S4. The addition of Pt indeed improved the activity and suppressed the formation of CH_4. Compared with $Pt\text{-}Ni/SiO_2$, the elimination of CH_4 production on Pt-Ni/NiPS is probably due to the efficient mass transfer between Pt and Ni^0 sites on the latter one.

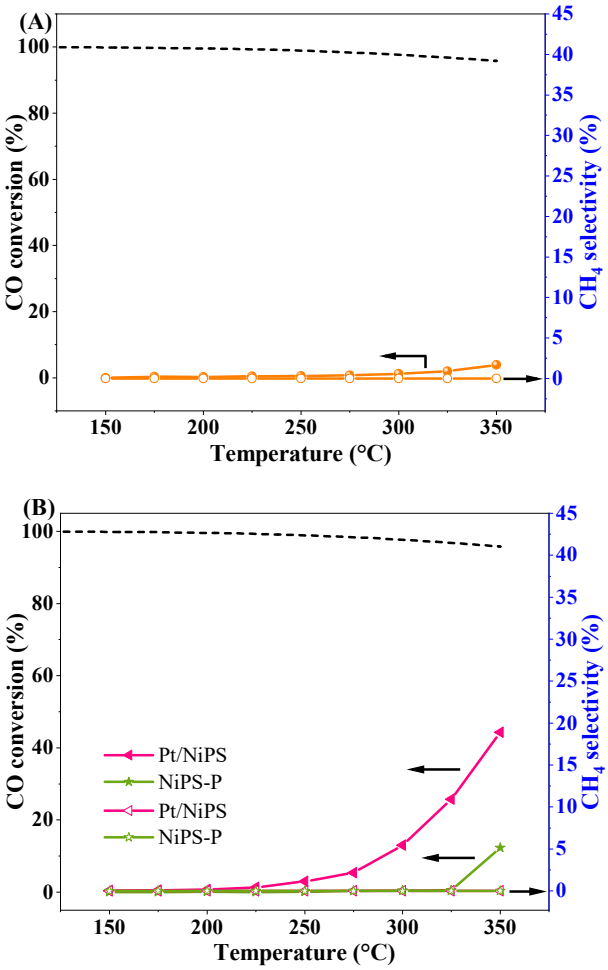

Fig. S5. CO conversion and CH_4 selectivity over (A) Pt/SiO_2, (B) Pt/NiPS and NiPS-P at WHSV = 36,000 mL g^{-1} h^{-1}. Dashed line: theoretical CO equilibrium conversion.

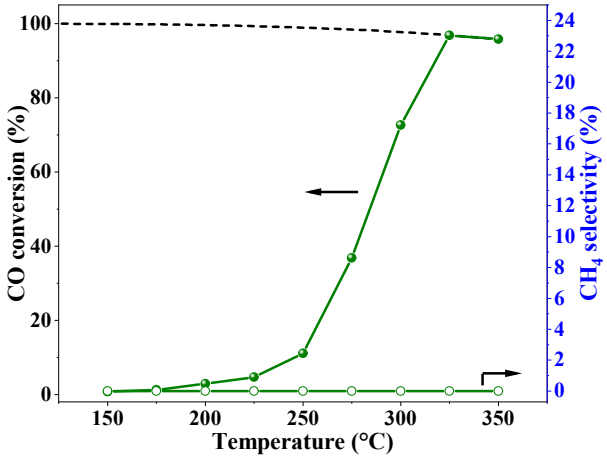

Fig. S6. CO conversion and CH_4 selectivity over Pt-Ni/NiPS at WHSV = 72,000 mL g^{-1} h^{-1}. Dashed line: theoretical CO equilibrium conversion.

Table S1. Textural properties of the samples

Sample	Pt content / wt.%[a]	Ni content / wt.%[a]	Surface area / $m^2\ g^{-1}$ [b]	Pore volume / mL g^{-1} [b]
NiPS-P	\	19.9	321.7	0.7
Pt/NiPS-P	0.5	19.5	311.6	0.8

[a] Determined by XRF analysis.

[b] Determined by BET analysis.

Table S2. Dispersion degree of Ni/NiPS and Pt-Ni/NiPS

Catalyst	*D* / %
Ni/NiPS	32.3
Pt-Ni/NiPS	30.3

According to the metal size distribution results shown in the TEM results, the dispersion degree (*D*) of Ni/NiPS and Pt-Ni/NiPS is 32.3% and 30.3%, respectively.

Table S3. XPS results of Ni/NiPS and Pt-Ni/NiPS

Catalyst	Pt^0 content / wt.%	$Ni^0/(Ni^0 + Ni^{2+})$
Ni/NiPS	\	0.024
Pt-Ni/NiPS	0.33	0.145

Table S4. The contrast of the catalysts for HT-WGSR

Catalyst	Condition	Temperature / °C	CO conversion / %	CH_4 selectivity / %	Reference
Pt-Ni/NiPS	5% CO/10% H_2O/85% N_2; WHSV = 36,000 mL g^{-1} h^{-1};	300[a]	98.7	0.0	This work
Pt-Ni/NiPS	5% CO/10% H_2O/85% N_2; WHSV = 72,000 mL g^{-1} h^{-1};	325[a]	96.8	0.0	This work
50Ni@TiO_{2-x}	6% CO/24% H_2O/70% Ar; WHSV = 66,000 mL g^{-1} h^{-1};	325[a]	100.0	5.0	6
15Ni/TiO_2	6% CO/24% H_2O/70% Ar; WHSV = 66,000 mL g^{-1} h^{-1};	450	39.0	2.0	6
7Ni-7.5Cu/CeO_2-Al_2O_3	18.8% CO/37.5 H_2O/37.5% H_2/6.2% CO_2; WHSV = 30,000 mL g^{-1} h^{-1};	400	55.0	5.7	7
10Ni/Al_2O_3	10% CO/20% H_2O/70% He; WHSV = 60,000 mL g^{-1} h^{-1};	350[a]	96.0	12.0	8
10Ni/2Na/CeO_2	5% CO/25% H_2O/70% He; GHSV = 68,000 h^{-1};	400[a]	97.5	1.0	9
5Ni-5Cu/CeO_2	5% CO/25% H_2O/70% He; GHSV = 68,000 h^{-1};	400[a]	94.5	1.0	10
10NiPS	5% CO/25% H_2O/70% He; GHSV = 68,000 h^{-1};	350[a]	95.8	0.6	11
10Ni/Zr-Ce-SBA-15	2% CO/10% H_2O/88% He; WHSV = 18,000 mL g^{-1} h^{-1};	400[a]	94.6	0.8	12
91.5Fe_3O_4-2.0Hg/6.5Cr_2O_3	50% H_2/12.5% CO/37.5 N_2; GHSV = 1,200,000 h^{-1}, P = 2.76 mPa;	400	37.4	\	13
62Fe-38CeO_x	H_2O : CO = 1.5; GHSV = 60,000 h^{-1};	550	71.0	0.0	14
92Fe-8Cr	H_2O : CO = 3.5; GHSV = 60,000 h^{-1};	450	75.0	\	15
74Fe/19Ce/7Cr	H_2O : CO = 3.5; GHSV = 60,000 h^{-1}.	500[a]	90.0	\	16

[a] Temperature reaching CO equilibrium conversion.

References

1 Z. Taherian, V. Shahed Gharahshiran, A. Khataee and Y. Orooji, *Fuel*, 2022, **311**, 122620.

2 M. Song, Z. Huang, B. Chen, S. Liu, S. Ullah, D. Cai and G. Zhan, *J. CO_2 Util.*, 2021, **52**, 101674.

3 R. Sawyer, H. Nesbitt and R. Secco, *J. Non. Cryst. Solids*, 2012, **358**, 290-302.

4 Y. Chen, J. Lin, L. Li, B. T. Qjao, J. Y. Liu, Y. Su and X. D. Wang, *ACS Catal.*, 2018, **8**, 859-868.

5 K. Ding, A. Gulec, A. M. Johnson, N. M. Schweitzer, G. D. Stucky, L. D. Marks and P. C. Stair, *Science*, 2015, **350**, 189-192.

6 M. Xu, S. He, H. Chen, G. Q. Cui, L. R. Zheng, B. Wang and M. Wei, *ACS Catal.*, 2017, **7**, 7600-7609.

7 N. S. Maboudi, F. Meshkani and M. Rezaei, *J. Energy Inst.*, 2021, **96**, 75-89.

8 J. Lin and V. V. Guliants, *ChemCatChem*, 2012, **4**, 1611-1621.

9 M. L. Ang, U. Oemar, E. T. Saw, L. Mo, Y. Kathiraser, B. H. Chia and S. Kawi, *ACS Catal.*, 2014, **4**, 3237-3248.

10 E. T. Saw, U. Oemar, X. R. Tan, Y. Du, A. Borgna, K. Hidajat and S. Kawi, *J. Catal.*, 2014, **314**, 32-46.

11 J. Ashok, M. L. Ang, P. Z. L. Terence and S. Kawi, *ChemCatChem*, 2016, **8**, 1308-1318.

12 P. Hongmanorom, J. Ashok, S. Das, N. Dewangan, Z. Bian, G. Mitchell, S. Xi, A. Borgna and S. Kawi, *J. Catal.*, 2020, **387**, 47-61.

13 C. Rhodes, B. Peter Williams, F. King and G. J. Hutchings, *Catal. Commun.*, 2002, **3**, 381-384.

14 D. Damma and P. G. Smirniotis, *Catalysts*, 2020, **10**, 639.

15 G. K. Reddy and P. G. Smirniotis, *Catal. Letters*, 2010, **141**, 27-32.

16 D. Devaiah and P. G. Smirniotis, *Ind. Eng. Chem. Res.*, 2017, **56**, 1772-1781.